



Supporting Online Material for

Compartmentalized Control of Skin Immunity by Resident Commensals

Shruti Naik, Nicolas Bouladoux, Christoph Wilhelm, Michael J. Molloy, Rosalba Salcedo, Wolfgang Kastenmuller, Clayton Deming, Mariam Quinones, Lily Koo, Sean Conlan, Sean Spencer, Jason A. Hall, Amiran Dzutsev, Heidi Kong, Daniel J. Campbell, Giorgio Trinchieri, Julia A. Segre, Yasmine Belkaid*

*To whom correspondence should be addressed. E-mail: ybelkaid@niaid.nih.gov

Published 26 July 2012 on *Science Express*
DOI: 10.1126/science.1225152

This PDF file includes:

Materials and Methods

Figs. S1 to S5

References

Materials and Methods

Mice

C57BL/6 specific pathogen-free mice were purchased from Taconic Farms and The Jackson Laboratory. Germ-free C57BL/6 mice were bred at Taconic Farms and maintained in the NIAID gnotobiotic facility. B6.129S1-*Tlr3*^{tm1Flv/J} (*Tlr3*^{-/-}), *Il-1r1*^{-/-}, and B6.129S7-*Rag1*^{tm1Mom} (*Rag1*^{-/-}) were obtained through the NIAID Taconic exchange program from Taconic Farms. B6.129S2-*Il6*^{tm1Kopf/J} (*Il-6*^{-/-}) mice were obtained from The Jackson Laboratory. *Il-23r*^{-/-} animals were a kind gift from Dr. M. Oukka (Seattle Children's Research Institute). B6.129-*Tlr2*^{tm1Kir/J} (*Tlr2*^{-/-}), B6.129P2-*Tlr5*^{tm1Aki} (*Tlr5*^{-/-}), B6.129P2-*Tlr9*^{tmAki} (*Tlr9*^{-/-}), B6.129P2-*Myd88*^{tmAki} (*Myd88*^{-/-}) and *Myd88*^{-/-}/*Ticam2*^{-/-} mice were generous gifts from Dr. A. Sher (NIAID/NIH). B6.129P2-*Il18*^{tmAki/J} (*Il-18*^{-/-}) and C57BL/9-*Tnfrsf1a*^{tm2.1Rsie} (*Tnfr1*^{-/-}) mice were obtained from Dr. G. Trinchieri (NCI/NIH) and Dr. R. Siegel (NIAMS/NIH), respectively. All mice were maintained at and all experiments were performed in an American Association for the Accreditation of Laboratory Animal Care-accredited animal facility at the National Institute for Allergy and Infectious Diseases (NIAID) and housed in accordance with the procedures outlined in the Guide for the Care and Use of Laboratory Animals under an animal study proposal approved by the NIAID Animal Care and Use Committee. Gender- and age-matched mice between 8-12 weeks of age were used.

Mouse tissue processing

Ears were excised and separated into the ventral and dorsal sheets. Flank (dorsal) skin was shaved with chrom mini (Wahl), adipose tissue was removed with a number 10 scalpel, and skin was cut in 1cm by 1cm pieces. Tissue samples were digested in RPMI containing 100 U/ml penicillin, 100 µg/ml streptomycin, 55 µM β-mercaptoethanol, 20 µM HEPES (HyClone), and 0.25 mg/ml Liberase purified enzyme blend (Roche Diagnostic Corp.), and incubated for 2 hours at 37°C and 5% CO₂. Digested skin sheets were homogenized using the Medicon/Medimachine tissue homogenizer system (Becton Dickinson). For isolation of keratinocytes, flank (dorsal) skin was shaved, adipose tissue was removed and skin was placed on 0.25% Trysin EDTA (Invitrogen) for 35-60 min at 37°C and 5% CO₂. Epidermal cells were manually scraped using a number 10 scalpel. Cells from spleen, the lymph nodes and the small intestine lamina propria were isolated as previously described (19).

Phenotypic analysis

Single cell suspensions were stained with either LIVE/DEAD Fixable Blue Dead Cell Stain Kit (Invitrogen) or 4', 6-diamidino-2-phenylindol (DAPI, Sigma) in HBSS to exclude dead cells. For detection of transcription factors, cells were stained using the Foxp3 staining set (eBioscience) according to the manufacturer's protocol. For detection of intracellular cytokines or langerin expression, cells were fixed and permeabilized with BD Cytofix/Cytoperm and stained in BD Perm Wash buffer (BD Biosciences). Cells were stained with the following antibodies purchased from either eBioscience, BD

Biosciences, or Dendritics corp: CD45.1 (A20), CD45.2 (104), $\gamma\delta$ TCR (GL3), TCR β (H57-57), CD4 (RM4-5), IL-10 (JES5-16E3), IL-17A (ebio17B7), IFN- γ (XMG1.2), TNF- α (MP6-XT22), Foxp3 (FJK-16a), Siglec-F (E50-2440), MHCII (M5/114.15.2) CD11b (M1/70), CD11c (N418), Fc ϵ RI (Mar-1), C-kit (2B8), Langerin (929F3.01), CD103 (2E7), α 6 (eBioGoH3), CD34 (RAM34), CD44 (IM7) and/or CD25 (PC61.5). Staining was performed in the presence of FcBlock (eBioscience), 0.2 mg/ml purified rat IgG and 1 mg/ml of normal mouse serum (Jackson Immunoresearch). Stain for skin homing markers was performed as previously described (34).

Immunofluorescence microscopy

Mouse skin samples were fixed in 10% formalin and paraffin embedded. Paraffin sections were dewaxed and washed with 95% ethanol followed by methanol hydrogen peroxide. The sections were then treated with a heat induced epitope retrieval (HIER) procedure using rodent Decloaker solution (Biocare Medical, RD913) and the Biocare decloaking chamber. After being washed in Tris pH 7.4, sections were incubated in the presence of rat serum and FcBlock (24G2) followed by rabbit anti-Escherichia coli B (DAKO, B0357) diluted in the blocking solution. Samples were washed in Tris and then incubated with goat anti-rabbit IgG-Texas Red antibody (Invitrogen, T2767). The tissue was then counterstained with HOECSHT, and imaged using a Leica DM IRBE fluorescent microscope.

Lymph nodes were harvested and fixed in 0.05 M PBS containing 0.1 M L-lysine (pH 7.4), 2 mg/ml NaIO₄, and 10mg/ml paraformaldehyde for 12 hrs. Samples were washed

in phosphate buffer and dehydrated in 30% sucrose phosphate buffer. Spleens were snap frozen in Tissue-Tek (Sakura Finetek). Sections were cut on cryostat. Lymphoid tissue samples were stained with LYVE-1 (Novus Biologicals), B220, CD4 (BD Biosciences), CD8 (Caltag), Collagen IV (Abcam), FDC-M2 (Immunokontakt) followed by secondary staining with goat anti-rabbit or goat anti-rat antibodies (Invitrogen).

Antibiotic treatment

Female 3-week-old C57BL/6 mice were provided ampicillin (1 g/l), vancomycin (500 mg/l), neomycin trisulfate (1 g/l), and metronidazole (1 g/l) in drinking water for 4 to 8 weeks as previously described (19) Mice were infected with *L. major* 4 weeks post-antibiotic treatment and maintained on antibiotics for the duration of the infection. All antibiotics were purchased from Sigma-Aldrich. Germ free animals were treated with vancomycin (500 mg/l) in drinking water starting one week prior to topical association with *S. epidermidis* maintained on antibiotic water for the duration of the experiment.

DNA extraction from skin and gut flora and 454 analysis

Ear and flank skin samples were sterilely obtained and processed using a protocol adapted from Grice et al (9). DNA was extracted from fecal pellets using QIAamp DNA stool mini kit (Qiagen). For quantitative analysis of 16S rDNA, real time PCR was performed using primers BacF (5'-CGGCAACGAGCGCAACCC-3') and BacR (5'-CCATTGTAGCACGTGTGTAGCC-3') (35). For sequencing of 16S rDNA amplicon libraries were prepared from sample DNA using Accuprime High Fidelity Taq

polymerase (Invitrogen) and universal primers flanking variable regions V1 (primer 27F; 5'-AGAGTTTGATCCTGGCTCAG-3') and V3 (primer 534R; 5'-ATTACCGCGGCTGCTGG-3'). For each sample, the universal primers were tagged with unique sequences ("barcodes") to allow for multiplexing/demultiplexing (36) PCR products were then purified using the Agencourt Ampure XP Kit (Beckman Counter Genomics) and quantitated using the QuantIT dsDNA High-Sensitivity Assay Kit (Invitrogen). Approximately equivalent amounts of each PCR product were then pooled and purified with a Qiagen minElute column (Qiagen) into 30 µl TE buffer prior to sequencing at the NIH Intramural Sequencing Center. Amplicon libraries were sequenced on a 454 FLX instrument using Titanium chemistry. Flowgrams were processed using the 454 Basecalling pipeline (v2.5.3). *Sequence pre-processing, alignment and chimera removal:* mothur (version 1.21.0)(37) was used for all 16S rRNA gene sequence analysis steps. Prior to analysis, sequences were trimmed of low quality ends and filtered to retain sequences with a minimum length of 200 bp. After alignment to a bacterial reference alignment (SILVA), chimeras were removed using the chimera slayer implementation in the mothur package. *Biodiversity and phylogenetic analyses:* From the alignment, a distance matrix was calculated and sequences were clustered into OTUs using the average neighbor algorithm at a cutoff of 0.03. Taxonomic classification of reads clustered in OTUs was done using the RDP Classifier included in mothur. A phylogenetic tree was generated from a relaxed neighbor-joining algorithm using the Clearcut program available via mothur. Unweighted and weighted UniFrac analyses (mothur & FastUnifrac <http://bmf.colorado.edu/fastunifrac/>) were subsequently done from the phylogenetic data

to evaluate community differences. Principal coordinate analysis (PCoA) was used to visualize distribution patterns from UniFrac distances.

Cohousing and microbial reconstitution

Wild-type age matched females were tail tattooed and housed in the same cage with equal number of respective knockout mice for at least two weeks. For association of germ-free mice with SFB (a kind gift from Dr. Yoshinori Umesaki (24)), fecal pellets isolated from SFB mono-associated mice were reconstituted in sterile PBS and 200 μ l of this suspension was administered to each germ-free mouse by gavage in sterile isolator. SFB reconstitution was confirmed by qPCR of fecal 16S rDNA relative to negative GF controls as previously described (38). Mono-associated mice were maintained for 1-2 weeks prior to analysis. For mono-association of germ-free mice with *Staphylococcus epidermidis*, clinical isolate NIHLM087 (9) was cultured for 18 hrs in tryptic soy broth at 37°C. Germ free mice were associated by placing 100 – 500 μ l of overnight *S. epidermidis* bacterial suspension on ear and flank skin using a sterile cotton swab every 3 days for one to two weeks. For infectious studies, mice were topically associated either a week prior or at time of *L. major* inoculation. *S. epidermidis* reconstitution was confirmed by sterilely homogenizing ear skin and plating on tryptic soy agar for 18 hrs.

ELISA

Naïve or infected skin tissue homogenates were cultured for 18 hrs in RPMI containing 100 U/ml penicillin, 100 μ g/ml streptomycin, 55 μ M β -mercaptoethanol, 20 μ M HEPES

(HyClone) and 10% FBS at 37°C. Supernatants were collected and levels of inflammatory mediators were measured either ELISA (R&D Systems) or multiplex (Millipore).

NanoString nCounter analysis

nCounter Gene Expression Assay was performed using two specific probes (capture and reporter) for each gene of interest. In brief, cell lysates from 10,000 cells per sample were hybridized with customized Reporter CodeSet and Capture ProbeSet according to manufacturer's instructions (NanoString Technologies, Seattle, USA), for direct labeling of mRNAs of interest with molecular barcodes without the use of reverse transcription or amplification. Then, the hybridized samples were recovered with the NanoString Prep Station and the mRNA molecules counted with the NanoString nCounter. The resulting counts were corrected by subtracting the average value of the negative control (alien probes from the CodeSet, lacking spiked transcript) from the raw counts obtained for each RNA. Values less than zero were considered equal to 1. The corrected raw data were finally normalized using *Gapdh* as housekeeping gene.

***Leishmania major* infection and parasite enumeration**

Mice were infected in the ear dermis with 10^4 - 10^5 *L. major* metacyclic promastigotes clone V1 (MHOM/IL/80/Friedlin) in a volume of 5 µl, using a 27 1/2 G needle as previously described (26) Lesion sizes were measured using an engineer caliper (Mitutoyo). To enumerate parasite, cytopsin slides prepared from single cell suspensions

of dermal lesions were stained with diff-quick (Fisher Scientific). Parasites and total number of nucleated on each slide were counted using a light microscope.

Generation of Bone Marrow Chimeras

Bone marrow was extracted from hind legs of knockout and wildtype animals and T cell depleted using CD90.2 microbeads (Miltenyi). 5 week old Rag1 deficient/ CD45.1 animals were lethally irradiated and reconstituted with either 10 million mixed WT: KO bone marrow cells in a 30: 70 ratio or individually into separate hosts (see figure S5H-I). Animals were maintained on antibiotics for up to one week after reconstitution. Cutaneous and intestinal lymphocytes were assessed 12-16 weeks after reconstitution.

***In vitro* T cell restimulation**

For detection of basal cytokine potential, single cell suspensions from various tissues were stimulated directly *ex vivo* with 50 ng/ml phorbol myristate acetate (PMA)/ (Sigma) and 5 µg/ml ionomycin (Sigma) in the presence of brefeldin A (GolgiPlug, BD Biosciences) in RPMI 1640 supplemented with 10% FBS, penicillin, streptomycin, HEPES, glutamine, nonessential amino acids, and 50 µM of β-mercaptoethanol for 4 hours at 37°C and 5% CO₂. For *Leishmania* specific stimulations, single cells suspensions were stimulated in the presence of soluble *Leishmania* antigen for 18 hrs. Brefeldin A (GolgiPlug, BD Biosciences) was added to cultures for the last 8 hrs. For *ex vivo* cytokine production analysis post *L. major* infection, skin tissue was digested in the presence of Brefeldin A and isolated cells were then incubated in the presence of

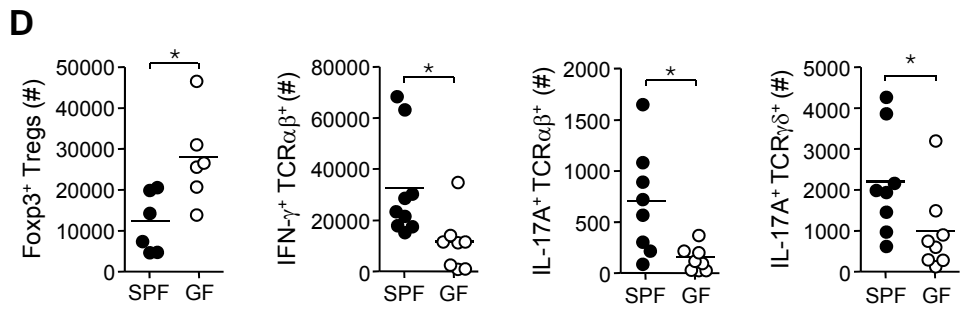
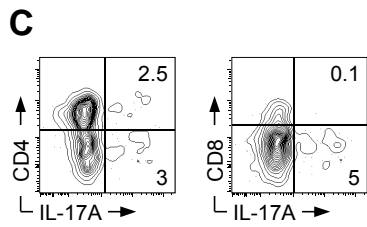
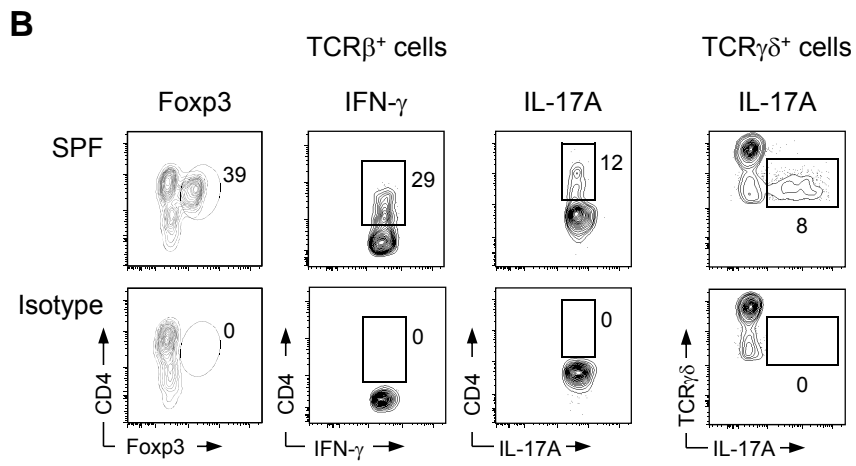
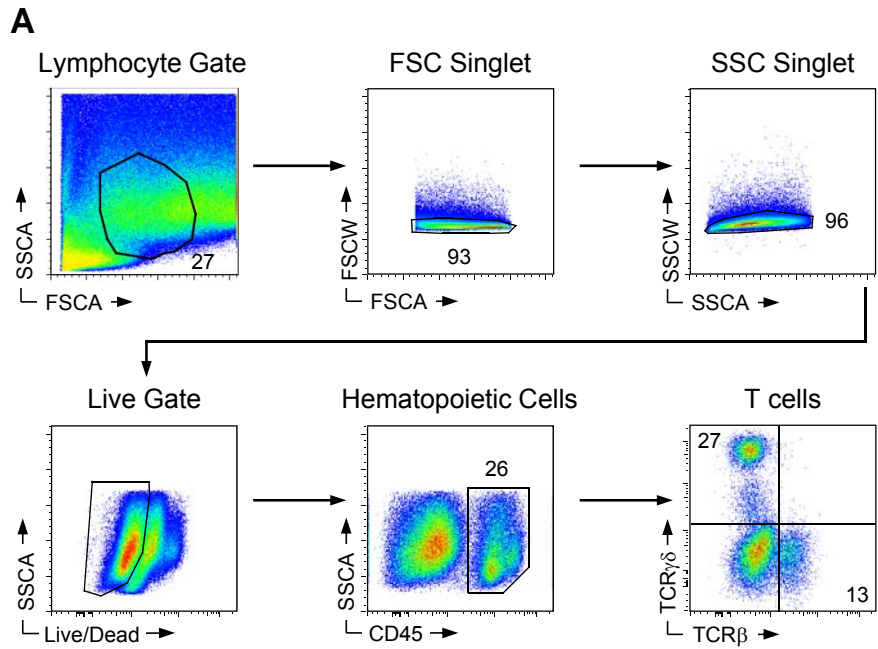
Brefeldin A and RPMI 1640 supplemented with 10% FBS, penicillin, streptomycin, HEPES, glutamine, nonessential amino acids, and 50 μ M of β -mercaptoethanol for 4 hrs at 37°C and 5% CO₂. CD4⁺ T cells, based on the expression of TCR β and CD4 and dermal $\gamma\delta$ T cells, based on intermediate expression levels of the pan $\gamma\delta$ TCR, were sorted from the skin of SPF mice. Purified cells T cells were cultured in α CD3 (1 μ g/ml) coated plates in the presence or absence of IL-1 α , IL-1 β (10ng/ml) or IL-6 (15 ng/ml) and supplemented with 10% FBS, penicillin, streptomycin, HEPES, glutamine, nonessential amino acids, and 50 μ M of β -mercaptoethanol for 48hrs at 37°C and 5% CO₂. Cytokine expression in the cell culture supernatants was assayed using FlowCytomix Multiplex Technology (ebioscience) and was adjusted to the plated density of 5x10³ cells in 50 μ l total culture volume.

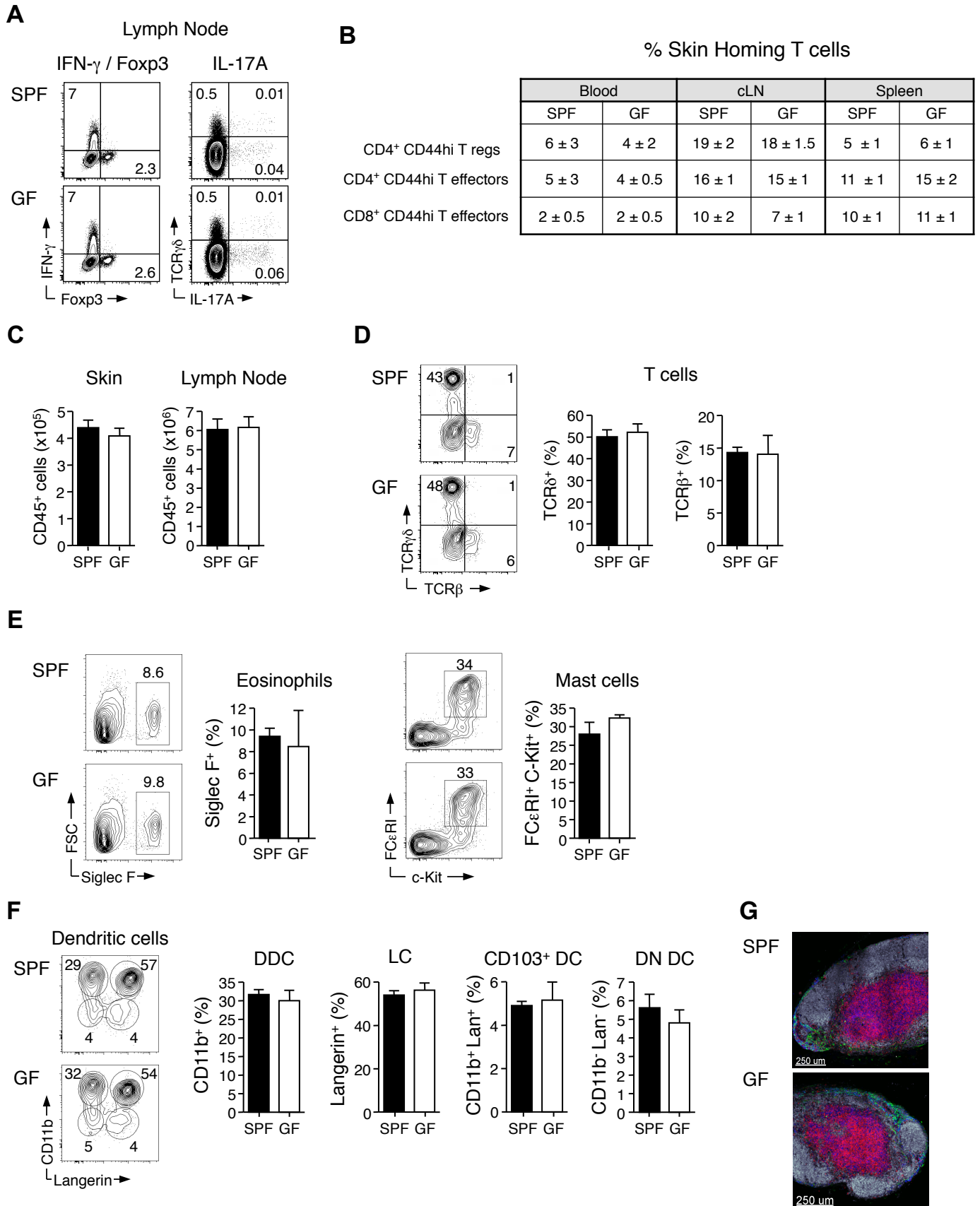
***In vivo* cytokine administration**

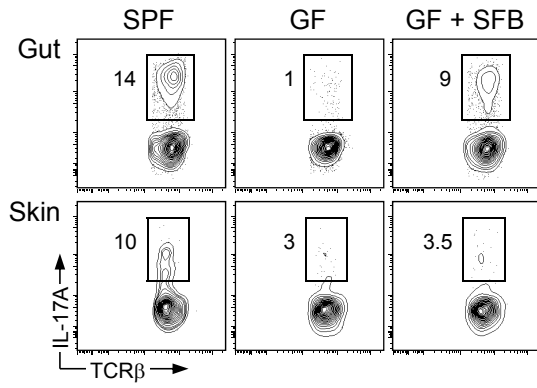
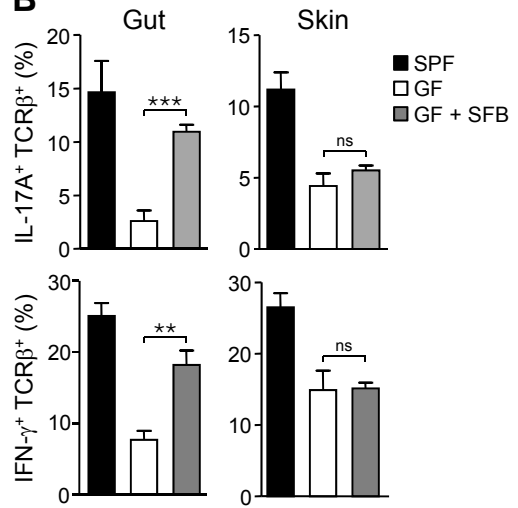
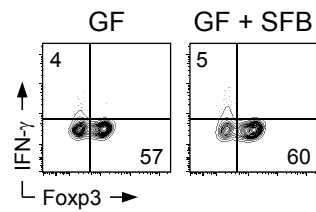
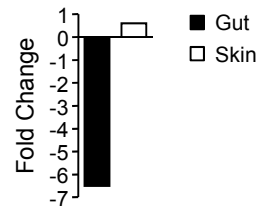
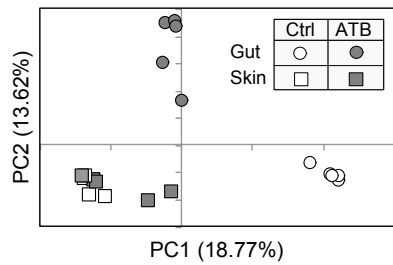
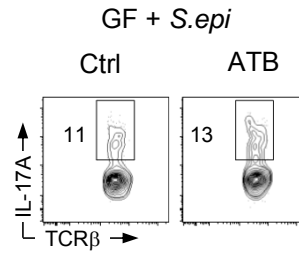
Naïve or *L. major* infected animals were treated intraperitoneally with either 250 mg/kg of recombinant human IL-1ra / Kineret (Biovitrum) or PBS control daily for 7 days starting at the time of infection and/or bacterial mono-association.

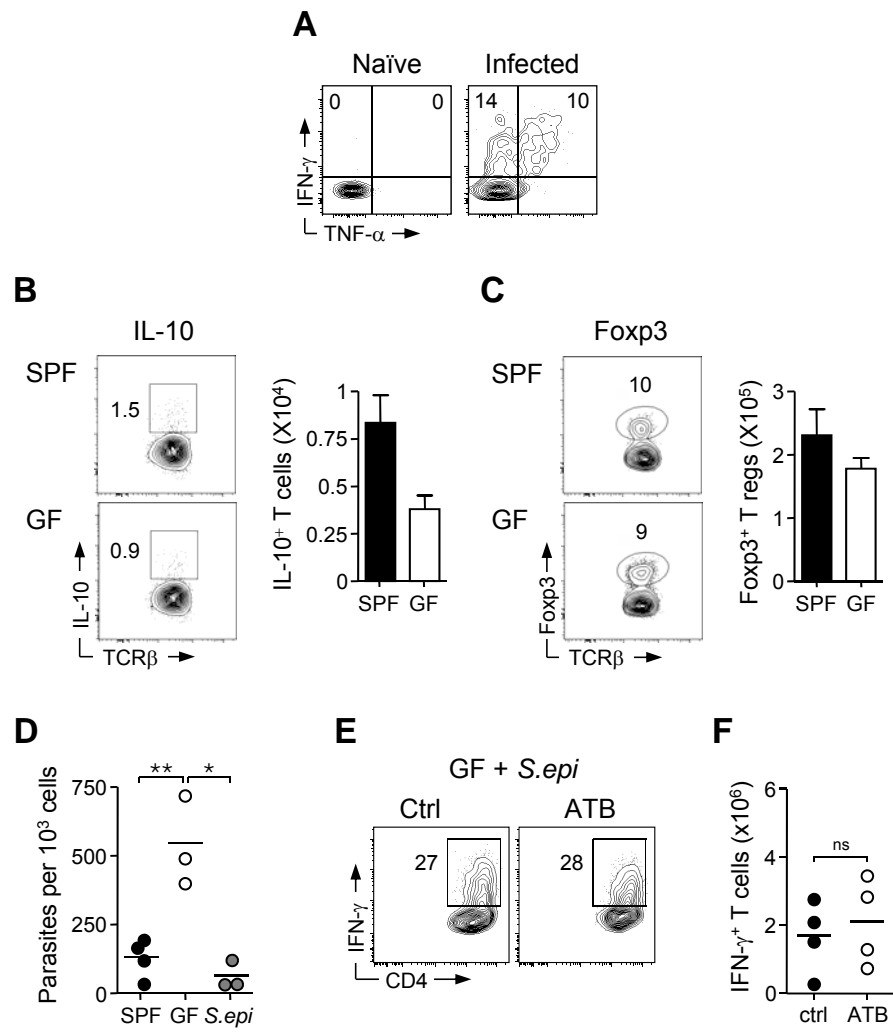
Statistics

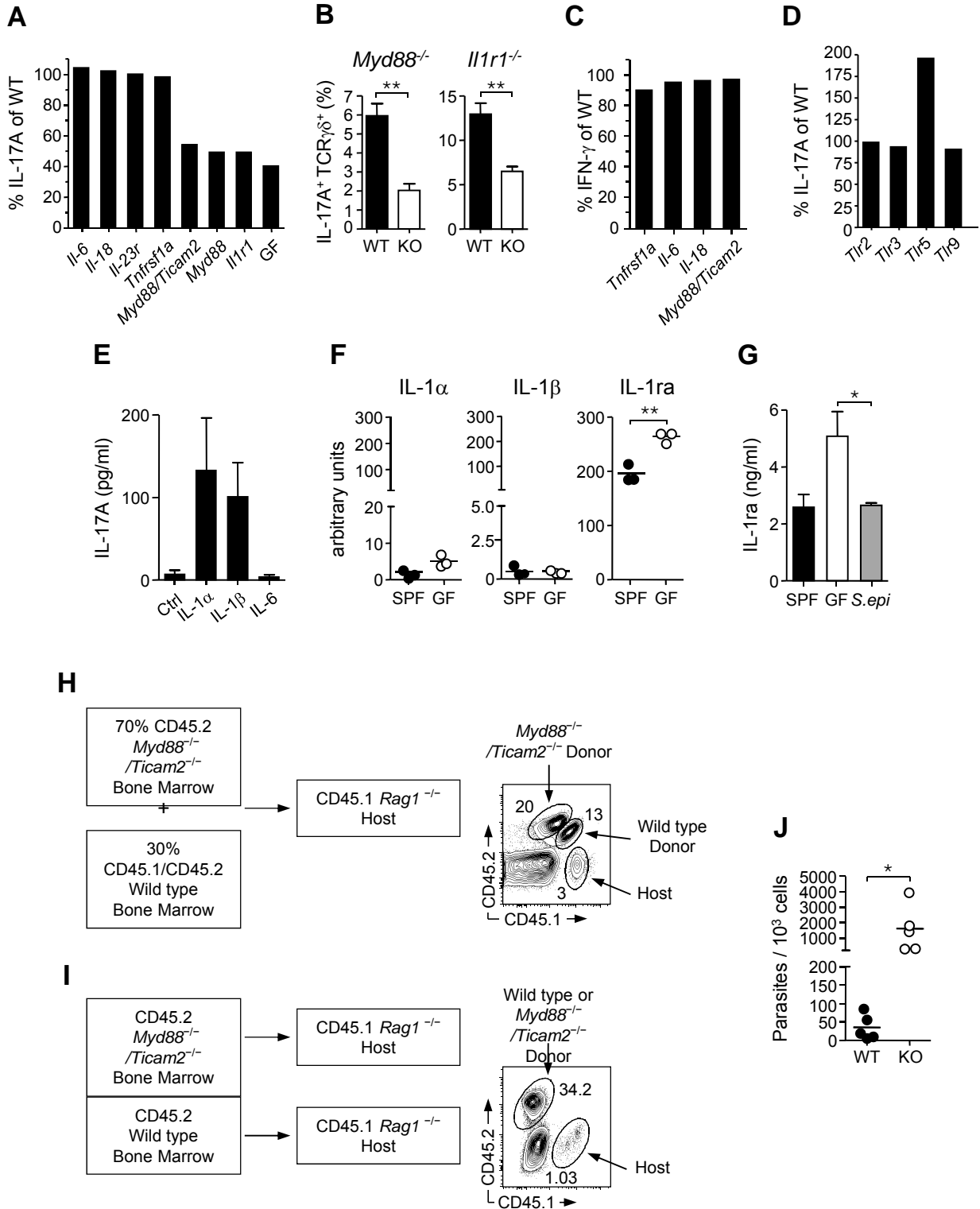
Unpaired Student *t* test was used to compare the corresponding populations. Error bars represent standard error of the mean.





A**B****C****D****E****F**





Supplementary Figure Legends

Fig. S1. (A) Gating strategy for T cells from skin tissue. (B) Representative plots of Foxp3 expression in live CD45⁺ TCRβ⁺ cells, IFN-γ and IL-17A expression in live CD45⁺ TCRβ⁺ cells, and IL-17A in live CD45⁺ TCRγδ⁺ cells and negative isotope control from skin tissue of SPF animals. (C) Representative plots of IL-17A expression by CD4⁺ and CD4 CD8 double negative TCRβ⁺ cells. (D) Numbers of Foxp3⁺ T_{regs}, IFN-γ⁺ and IL-17A⁺ TCRβ⁺ cells, and IL-17A⁺ TCRγδ⁺ from skin tissue of SPF (●) and GF (○) mice. Results are a compilation of 3-5 experiments (*p< 0.05)

Fig. S2. (A) Representative plots of IFN-γ, and Foxp3 expression in live CD45⁺ TCRβ⁺ CD4⁺ cells and IL-17A expression in live CD45⁺ cells extracted from cutaneous lymph nodes of SPF (■) and GF (□) mice post PMA/ Ionomycin stimulation. Results are representative of 3 experiments. (B) Summary of skin homing markers expressed by T cells in from blood, cutaneous lymph node, and spleen of SPF and GF mice. Skin homing subsets were defined as follows: CD44^{hi} CD4⁺ T_{regs} and T effectors were evaluated for CD103 and high P-selectin ligand surface expression and CD44^{hi} CD8⁺ T effectors were analyzed for high P-selectin ligand surface expression. Results are representative of 2 experiments. (C) Quantification of total CD45⁺ hematopoietic cells from the skin and associated lymph node of SPF (■) and GF (□) mice. Error bar is a mean of 4 mice ± SEM. Results are representative of 3 experiments. (D) Frequency of TCRγδ⁺ and TCRβ⁺

subsets from the skin tissue of SPF (■) and GF (□) mice Error bar is a mean of 4 mice \pm SEM. Results are representative of 3 experiments. (E-F) Summarized proportions of eosinophils, mast cells, and various dendritic cell subsets from skin tissue of SPF (■) and GF (□) mice. Gating strategy for various dendritic cell subsets in skin. Cells are gated on live CD45⁺ CD11c⁺ and MHCII⁺. Subsets are defined as follows: Langerin cell (16) are gated on CD11b⁺ CD207⁺ (Langerin) cells, Langerin⁺ Skin DC (CD103 DC) are gated on CD11b⁻ CD103⁺ cells, Skin Dendritic cell (DDC) gated on Langerin⁻ CD11b⁻ cells and double negative skin dendritic cells (DNDC) are gated on CD11b⁻ Langerin⁻. Error bar is a mean of 4 mice \pm SEM. Results are representative of 2-3 experiments. (G) Representative images of retroauricular lymph node sections from naïve SPF and GF mice immunolabeled with anti-B220 (White; labels B cells), CD8 (Red) CD4 (Blue) and Collagen IV (Green). Results are representative of 2 experiments.

Fig. S3. (A-B) Comparative analysis of IL-17A and IFN- γ expression in intestine and skin of SPF, GF, and GF mice mono-associated with Segmented Filamentous Bacteria (SFB). Flow cytometry plots are gated on live CD45⁺ TCR β ⁺ cells. (***) $p < 0.0005$. Results are representative of 2 experiments. (C) Representative plots of IFN- γ and Foxp3 expression in the skin of SPF, and GF mice mono-associated with Segmented Filamentous Bacteria (SFB). Plots gated on live CD45⁺ TCR β ⁺ cells. Results are representative of 2 experiments. (D) Quantification of 16S rDNA copies in the skin tissue and fecal pellet of mice treated with oral antibiotic (ATB) or water control (Ctrl). Results are representative of 2 experiments. (E) Taxonomic affiliations at the phyla levels of 16S

rRNA gene sequence data clustered at 97% identity from skin tissue and fecal pellet of control and antibiotic treated mice. Principal coordinate analysis (PCoA) of unweighted pairwise UniFrac distances from a phylogenetic tree of unique reads. **(F)** Representative plots from GF mice associated with *S. epidermidis* and treated with oral vancomycin (ATB) or unsupplemented water (Ctrl). Results are representative of 1 experiment with 4 mice per group.

Fig. S4. **(A)** Representative plots of Leishmania antigen specific IFN- γ and TNF- α production by live CD45⁺TCR β ⁺ CD4⁺ dermal cells from naïve and *L. major* infected skin tissue of SPF animals. **(B)** Analysis of Leishmania specific IL-10 production by live CD45⁺ TCR β ⁺ CD4⁺ cells from SPF (●) and GF (○) mice. Each bar is a mean of 10 mice \pm SEM. Results are representative of 3 experiments. **(C)** Frequency of regulatory T cells (live CD45⁺ TCR β ⁺ CD4⁺ Foxp3⁺) in *L. major* infected skin lesions of SPF (●) and GF (○) mice. Each bar is a mean of 4 mice \pm SEM. Results are representative of 3 experiments. **(D)** Number of *L. major* parasites per 1000 nucleated cells from dermal lesions of infected SPF (●), GF (○), and GF mice mono-associated with *Staphylococcus epidermidis* (GF +*S.epi* (●)). Results are representative of 2 experiments. Each data point represents an individual mouse (*p< 0.05, **p< 0.005). **(E-F)** Assessment of *Leishmania* specific IFN- γ specific production by TCR β ⁺ CD4⁺ in GF + *S. epi* mice treated with either oral vancomycin (ATB (○)) or water (Ctrl (●)). Each data point represents an individual mouse. Results are representative of 1 experiment.

Fig. S5. (A) Expression of IL-17A by live CD45⁺ skin cells from various knockout mice relative to wild type control mice. Each bar is representative of 2-3 experiments with 2 to 4 mice per groups. (B) IL-17A production by live CD45⁺ TCR γ δ ⁺ cells from the skin of age matched *Myd88*^{-/-} and *Il1r1*^{-/-} mice. Error bar is a mean of 3-4 mice \pm SEM (**p< 0.005). Results are representative of 2-3 experiments. (C) Expression of IFN- γ by live CD45⁺ TCR β ⁺ skin cells from various knockout mice relative to wild type controls. Each bar is representative of 2-5 experiments. (D) Expression of IL-17A by live CD45⁺ skin cells from *Tlr2*, *Tlr3*, *Tlr5* and *Tlr9*^{-/-} mice relative to wild type control mice. Each bar is representative of 2-3 experiments with 2 to 4 mice per groups. (E) Assessment of IL-17A production from purified dermal TCR γ δ ^{low} cultured *in vitro* in the presence of anti-CD3 and either IL-1 α , IL-1 β or IL-6. Error bar is a mean of 3 experimental groups \pm SEM (*p< 0.05). Results are representative of 3 experiments. (F) Gene expression analysis of IL-1 α , IL-1 β and IL-1ra in interfollicular α 6⁺ keratinocytes from SPF (●) and GF (○) using NanoString nCounter analysis (**p< 0.005). (G) Spontaneous release of IL-1ra from skin derived cells of naïve SPF (■), GF (□), and GF + *S.epi* (▀) mice as measured by ELISA (*p< 0.05). (H-I) Schematic for generation of bone marrow chimeras to evaluate immune cells in the skin. Gating strategy for identifying wild type (WT) and *Myd88*^{-/-}/*Ticam2*^{-/-} cells in skin of bone marrow chimeric mice. (J) Number of *L. major* parasites per 1000 nucleated cells from dermal lesions of infected WT (●) and *Myd88*^{-/-}/*Ticam2*^{-/-} (○) mice. Each data point represents an individual mouse (*p< 0.05).

References

1. Y. K. Lee, S. K. Mazmanian, Has the microbiota played a critical role in the evolution of the adaptive immune system? *Science* **330**, 1768 (2010). [doi:10.1126/science.1195568](https://doi.org/10.1126/science.1195568) [Medline](#)
2. C. Huttenhower *et al.*; Human Microbiome Project Consortium, Structure, function and diversity of the healthy human microbiome. *Nature* **486**, 207 (2012). [doi:10.1038/nature11234](https://doi.org/10.1038/nature11234) [Medline](#)
3. B. A. Methé *et al.*; Human Microbiome Project Consortium, A framework for human microbiome research. *Nature* **486**, 215 (2012). [doi:10.1038/nature11209](https://doi.org/10.1038/nature11209) [Medline](#)
4. T. Ichinohe *et al.*, Microbiota regulates immune defense against respiratory tract influenza A virus infection. *Proc. Natl. Acad. Sci. U.S.A.* **108**, 5354 (2011). [doi:10.1073/pnas.1019378108](https://doi.org/10.1073/pnas.1019378108) [Medline](#)
5. J. J. Cebra, Influences of microbiota on intestinal immune system development. *Am. J. Clin. Nutr.* **69**, 1046S (1999). [Medline](#)
6. T. B. Clarke *et al.*, Recognition of peptidoglycan from the microbiota by Nod1 enhances systemic innate immunity. *Nat. Med.* **16**, 228 (2010). [doi:10.1038/nm.2087](https://doi.org/10.1038/nm.2087) [Medline](#)
7. Y. K. Lee, J. S. Menezes, Y. Umesaki, S. K. Mazmanian, Proinflammatory T-cell responses to gut microbiota promote experimental autoimmune encephalomyelitis. *Proc. Natl. Acad. Sci. U.S.A.* **108** (suppl. 1), 4615 (2011). [doi:10.1073/pnas.1000082107](https://doi.org/10.1073/pnas.1000082107) [Medline](#)
8. H. J. Wu *et al.*, Gut-residing segmented filamentous bacteria drive autoimmune arthritis via T helper 17 cells. *Immunity* **32**, 815 (2010). [doi:10.1016/j.immuni.2010.06.001](https://doi.org/10.1016/j.immuni.2010.06.001) [Medline](#)
9. E. A. Grice *et al.*, Topographical and temporal diversity of the human skin microbiome. *Science* **324**, 1190 (2009). [doi:10.1126/science.1171700](https://doi.org/10.1126/science.1171700) [Medline](#)
10. E. K. Costello *et al.*, Bacterial community variation in human body habitats across space and time. *Science* **326**, 1694 (2009). [doi:10.1126/science.1177486](https://doi.org/10.1126/science.1177486) [Medline](#)
11. R. L. Gallo, T. Nakatsuji, Microbial symbiosis with the innate immune defense system of the skin. *J. Invest. Dermatol.* **131**, 1974 (2011). [doi:10.1038/jid.2011.182](https://doi.org/10.1038/jid.2011.182) [Medline](#)

12. H. H. Kong *et al.*; NISC Comparative Sequence Program, Temporal shifts in the skin microbiome associated with disease flares and treatment in children with atopic dermatitis. *Genome Res.* **22**, 850 (2012). [doi:10.1101/gr.131029.111](https://doi.org/10.1101/gr.131029.111) [Medline](#)
13. Y. Lai *et al.*, Commensal bacteria regulate Toll-like receptor 3-dependent inflammation after skin injury. *Nat. Med.* **15**, 1377 (2009). [doi:10.1038/nm.2062](https://doi.org/10.1038/nm.2062) [Medline](#)
14. E. A. Grice, J. A. Segre, The skin microbiome. *Nat. Rev. Microbiol.* **9**, 244 (2011). [doi:10.1038/nrmicro2537](https://doi.org/10.1038/nrmicro2537) [Medline](#)
15. Y. Belkaid, C. A. Piccirillo, S. Mendez, E. M. Shevach, D. L. Sacks, CD4⁺CD25⁺ regulatory T cells control *Leishmania major* persistence and immunity. *Nature* **420**, 502 (2002). [doi:10.1038/nature01152](https://doi.org/10.1038/nature01152) [Medline](#)
16. N. Sumaria *et al.*, Cutaneous immunosurveillance by self-renewing dermal $\gamma\delta$ T cells. *J. Exp. Med.* **208**, 505 (2011). [doi:10.1084/jem.20101824](https://doi.org/10.1084/jem.20101824) [Medline](#)
17. D. A. Hill *et al.*, Metagenomic analyses reveal antibiotic-induced temporal and spatial changes in intestinal microbiota with associated alterations in immune cell homeostasis. *Mucosal Immunol.* **3**, 148 (2010). [doi:10.1038/mi.2009.132](https://doi.org/10.1038/mi.2009.132) [Medline](#)
18. I. I. Ivanov *et al.*, Induction of intestinal Th17 cells by segmented filamentous bacteria. *Cell* **139**, 485 (2009). [doi:10.1016/j.cell.2009.09.033](https://doi.org/10.1016/j.cell.2009.09.033) [Medline](#)
19. J. A. Hall *et al.*, Commensal DNA limits regulatory T cell conversion and is a natural adjuvant of intestinal immune responses. *Immunity* **29**, 637 (2008). [doi:10.1016/j.immuni.2008.08.009](https://doi.org/10.1016/j.immuni.2008.08.009) [Medline](#)
20. N. S. Wilson *et al.*, Normal proportion and expression of maturation markers in migratory dendritic cells in the absence of germs or Toll-like receptor signaling. *Immunol. Cell Biol.* **86**, 200 (2008). [doi:10.1038/sj.icb.7100125](https://doi.org/10.1038/sj.icb.7100125) [Medline](#)
21. M. Guilliams *et al.*, Skin-draining lymph nodes contain dermis-derived CD103⁻ dendritic cells that constitutively produce retinoic acid and induce Foxp3⁺ regulatory T cells. *Blood* **115**, 1958 (2010). [doi:10.1182/blood-2009-09-245274](https://doi.org/10.1182/blood-2009-09-245274) [Medline](#)
22. L. Wen *et al.*, Innate immunity and intestinal microbiota in the development of Type 1 diabetes. *Nature* **455**, 1109 (2008). [doi:10.1038/nature07336](https://doi.org/10.1038/nature07336) [Medline](#)

23. I. I. Ivanov *et al.*, Specific microbiota direct the differentiation of IL-17-producing T-helper cells in the mucosa of the small intestine. *Cell Host Microbe* **4**, 337 (2008).
[doi:10.1016/j.chom.2008.09.009](https://doi.org/10.1016/j.chom.2008.09.009) [Medline](#)
24. Y. Umesaki, Y. Okada, S. Matsumoto, A. Imaoka, H. Setoyama, Segmented filamentous bacteria are indigenous intestinal bacteria that activate intraepithelial lymphocytes and induce MHC class II molecules and fucosyl asialo GM1 glycolipids on the small intestinal epithelial cells in the ex-germ-free mouse. *Microbiol. Immunol.* **39**, 555 (1995).
[Medline](#)
25. S. Rakoff-Nahoum, J. Paglino, F. Eslami-Varzaneh, S. Edberg, R. Medzhitov, Recognition of commensal microflora by toll-like receptors is required for intestinal homeostasis. *Cell* **118**, 229 (2004). [doi:10.1016/j.cell.2004.07.002](https://doi.org/10.1016/j.cell.2004.07.002) [Medline](#)
26. Y. Belkaid *et al.*, A natural model of *Leishmania major* infection reveals a prolonged “silent” phase of parasite amplification in the skin before the onset of lesion formation and immunity. *J. Immunol.* **165**, 969 (2000). [Medline](#)
27. M. R. de Oliveira *et al.*, Influence of microbiota in experimental cutaneous leishmaniasis in Swiss mice. *Rev. Inst. Med. Trop. Sao Paulo* **41**, 87 (1999). [doi:10.1590/S0036-46651999000200005](https://doi.org/10.1590/S0036-46651999000200005) [Medline](#)
28. C. E. Sutton *et al.*, Interleukin-1 and IL-23 induce innate IL-17 production from gammadelta T cells, amplifying Th17 responses and autoimmunity. *Immunity* **31**, 331 (2009).
[doi:10.1016/j.immuni.2009.08.001](https://doi.org/10.1016/j.immuni.2009.08.001) [Medline](#)
29. L. Guo *et al.*, IL-1 family members and STAT activators induce cytokine production by Th2, Th17, and Th1 cells. *Proc. Natl. Acad. Sci. U.S.A.* **106**, 13463 (2009).
[doi:10.1073/pnas.0906988106](https://doi.org/10.1073/pnas.0906988106) [Medline](#)
30. M. H. Shaw, N. Kamada, Y. G. Kim, G. Núñez, Microbiota-induced IL-1 β , but not IL-6, is critical for the development of steady-state TH17 cells in the intestine. *J. Exp. Med.* **209**, 251 (2012). [doi:10.1084/jem.20111703](https://doi.org/10.1084/jem.20111703) [Medline](#)
31. W. Hu, T. D. Troutman, R. Edukulla, C. Pasare, Priming microenvironments dictate cytokine requirements for T helper 17 cell lineage commitment. *Immunity* **35**, 1010 (2011).
[doi:10.1016/j.immuni.2011.10.013](https://doi.org/10.1016/j.immuni.2011.10.013) [Medline](#)

32. L. S. Miller *et al.*, MyD88 mediates neutrophil recruitment initiated by IL-1R but not TLR2 activation in immunity against *Staphylococcus aureus*. *Immunity* **24**, 79 (2006).
[doi:10.1016/j.immuni.2005.11.011](https://doi.org/10.1016/j.immuni.2005.11.011) [Medline](#)
33. J. E. Sims, D. E. Smith, The IL-1 family: regulators of immunity. *Nat. Rev. Immunol.* **10**, 89 (2010). [doi:10.1038/nri2691](https://doi.org/10.1038/nri2691) [Medline](#)
34. J. C. Dudda, N. Perdue, E. Bachtanian, D. J. Campbell, Foxp3+ regulatory T cells maintain immune homeostasis in the skin. *J. Exp. Med.* **205**, 1559 (2008).
[doi:10.1084/jem.20072594](https://doi.org/10.1084/jem.20072594) [Medline](#)
35. C. X. Pei *et al.*, Diversity and abundance of the bacterial 16S rRNA gene sequences in forestomach of alpacas (*Lama pacos*) and sheep (*Ovis aries*). *Anaerobe* **16**, 426 (2010).
[doi:10.1016/j.anaerobe.2010.06.004](https://doi.org/10.1016/j.anaerobe.2010.06.004) [Medline](#)
36. N. J. Lennon *et al.*, A scalable, fully automated process for construction of sequence-ready barcoded libraries for 454. *Genome Biol.* **11**, R15 (2010). [doi:10.1186/gb-2010-11-2-r15](https://doi.org/10.1186/gb-2010-11-2-r15)
[Medline](#)
37. P. D. Schloss *et al.*, Introducing mothur: open-source, platform-independent, community-supported software for describing and comparing microbial communities. *Appl. Environ. Microbiol.* **75**, 7537 (2009). [doi:10.1128/AEM.01541-09](https://doi.org/10.1128/AEM.01541-09) [Medline](#)
38. N. H. Salzman *et al.*, Enteric defensins are essential regulators of intestinal microbial ecology. *Nat. Immunol.* **11**, 76 (2010). [doi:10.1038/ni.1825](https://doi.org/10.1038/ni.1825) [Medline](#)